Applied Physics Letters

Crystal orientation dependence of spin-orbit torques in Co/Pt bilayers

Cite as: Appl. Phys. Lett. **114**, 142402 (2019); https://doi.org/10.1063/1.5090610
Submitted: 29 January 2019 . Accepted: 22 March 2019 . Published Online: 10 April 2019

Jeongchun Ryu, Can Onur Avci, Shutaro Karube, Makoto Kohda, Geoffrey S. D. Beach, and Junsaku Nitta

View Online Export Citation CrossMark

ARTICLES YOU MAY BE INTERESTED IN

Recent advances in spin-orbit torques: Moving towards device applications
Applied Physics Reviews **5**, 031107 (2018); https://doi.org/10.1063/1.5041793

Anomalous spin Hall magnetoresistance in Pt/Co bilayers
Applied Physics Letters **112**, 202405 (2018); https://doi.org/10.1063/1.5021510

Spin transfer torque devices utilizing the giant spin Hall effect of tungsten
Applied Physics Letters **101**, 122404 (2012); https://doi.org/10.1063/1.4753947

Lock-in Amplifiers
Find out more today

Zurich Instruments

AIP Publishing

© 2019 Author(s).

Applied Physics Letters ARTICLE scitation.org/journal/apl

Crystal orientation dependence of spin-orbit torques in Co/Pt bilayers

Cite as: Appl. Phys. Lett. **114**, 142402 (2019); doi: 10.1063/1.5090610
Submitted: 29 January 2019 · Accepted: 22 March 2019 ·
Published Online: 10 April 2019

View Online Export Citation CrossMark

Jeongchun Ryu,[1,2,a)] Can Onur Avci,[2,b)] Shutaro Karube,[1] Makoto Kohda,[1,3,4] Geoffrey S. D. Beach,[2] and Junsaku Nitta[1,3,4,c)]

AFFILIATIONS

[1]Department of Materials Science, Tohoku University, Sendai 980-8579, Japan
[2]Department of Materials Science and Engineering, Massachusetts Institute of Technology, Cambridge, Massachusetts 02139, USA
[3]Spintronics Research Network, Tohoku University, Sendai 980-8579, Japan
[4]Organization for Advanced Studies, Center for Science and Innovation in Spintronics (Core Research Cluster), Tohoku University, Sendai 980-8579, Japan

[a)]**Present address:** Department of Materials Science, KAIST, Daejeon, South Korea.
[b)]**Present address:** Department of Materials, ETH Zürich, CH-8093 Zürich, Switzerland.
[c)]**E-mail:** nitta@material.tohoku.ac.jp

ABSTRACT

We study the role of Pt crystal orientation in spin-orbit torques in Co/Pt bilayers by means of the harmonic Hall effect and current-induced switching measurements. Perpendicularly magnetized Co/Pt bilayers were fabricated with the Pt layer exhibiting either a polycrystalline grain structure or an epitaxial (111)-oriented film on MgO substrates by magnetron sputtering. We find that the damping-like spin-orbit torque is 1.3 times smaller in the epitaxial Co/Pt(111) bilayers compared to the polycrystalline films, whereas the field-like spin-orbit torque values are of comparable magnitude. Current-induced magnetization switching measurements show good agreement with the results of harmonic measurements of damping-like torque, i.e., the critical switching current is about 30% higher in epitaxial Co/Pt(111). These results highlight the importance of crystal orientation effects on spin-orbit torques in nominally identical bilayer structures.

Published under license by AIP Publishing. https://doi.org/10.1063/1.5090610

In ferromagnet/heavy metal (FM/HM) bilayers with large spin-orbit coupling, charge current injection generates current-induced torques on the ferromagnet due to bulk (spin Hall) and interfacial (Rashba-type) effects. These spin-orbit torques (SOTs) can switch the magnetization and manipulate the magnetic textures such as domain walls in both in-plane and perpendicularly magnetized heterostructures.[1–7] Due to the technological relevance and fundamental interest, a wide variety of FM and HM combinations have been examined.[3,7–12] Among these, Co/Pt is considered as one of the model heterostructures in SOT studies due to the perpendicular magnetic anisotropy and the strong spin-orbit coupling inherent to this system.[1,13–17] It has been revealed that in FM/Pt bilayers, the spin Hall effect (SHE) of Pt[18–23] provides a major contribution to the SOTs.[16,17] Considering that the spin relaxation mechanism in Pt depends on its crystal structure,[24–26] one may expect that the SOTs induced by Pt likewise depend on the crystallographic texture and the grain morphology. For instance, the Elliot-Yafet mechanism[27,28] can be modulated by periodic crystal structures, producing different SHE depending on the direction of charge current relative to the crystal symmetry directions. Likewise, the Rashba effect in metal systems might also generate distinct effective magnetic fields depending on the Pt crystallographic orientation.

In this Letter, we investigate the dependence of current-induced SOTs in Co/Pt bilayers on the crystal structure of the Pt layer. Current-induced effective magnetic fields are evaluated using harmonic Hall voltage measurements. The damping-like (DL) torque is found to be lower when Co is grown on an epitaxial Pt film as opposed to a polycrystalline Pt layer. On the other hand, the field-like (FL) torque has a comparable value in both films. Current-induced magnetization switching measurements reveal critical currents whose relative magnitudes are in agreement with different DL-SOT strengths.

We sputtered AlOx(2 nm)/Co(1 nm)/Pt(5 nm) layers on single crystal MgO(100) and MgO(111) substrates. To obtain the desired epitaxy, we heated the substrate and kept the temperature at 200 °C during the Pt deposition.[24,29,30] The substrate was then allowed to cool to room temperature before subsequent deposition of the Co film to minimize interfacial mixing. Finally, an AlOx capping layer was grown at

Published under license by AIP Publishing

room temperature. X-ray diffraction (XRD) measurements in symmetric θ-2θ geometry were performed to evaluate the crystal structure as shown in Fig. 1(a). We observe that the XRD spectra of layers grown on MgO(111) exhibit only Pt(111) peaks, indicating epitaxial (111) growth templated by the MgO substrate. On the other hand, we observe both Pt(100) and Pt(111) peaks in the XRD spectra of films grown on MgO(100), indicating a polycrystalline film structure with no preferred crystallographic orientation. Furthermore, the peaks of Pt(111) on the MgO(100) substrate are broader than that in the Pt grown on MgO(111), evidencing the distorted structure of Pt(111) in the former. These suggest that Pt on MgO(100) cannot follow the substrates' structures fully and relaxes to the more energetically favorable bulk phase of (111) after a few monolayers. Co films tend to have (001) orientation which has the same structure as Pt(111). Therefore, we conclude that the entire Co/Pt bilayer is epitaxial on MgO(111), and for the layers grown on MgO(100), Co and Pt near the Co interface are polycrystalline (see supplementary material). In the text below, we denote the epitaxial film grown on MgO(111) as "epi-Co/Pt" and the polycrystalline film grown on MgO(100) as "poly-Co/Pt."

Polar magneto-optical Kerr effect measurements on continuous films show square hysteresis loops with coercivity of the order of 50 mT, confirming perpendicular magnetic anisotropy (PMA) in both samples [Fig. 1(b)]. Similarly, the prepared films were patterned into 5 μm-wide symmetric Hall cross structures using standard photolithography and Ar ion milling. Figure 1(c) schematically shows the device and measurement geometry, including coordinate system definitions. The resistivity is found to be 29 $\mu\Omega$ cm for poly-Co/Pt and 23 $\mu\Omega$ cm for epi-Co/Pt, with the difference being attributed to reduced bulk scattering due to high structural order on the latter. In order to evaluate SOTs, we performed harmonic Hall voltage measurements with an a.c. current density amplitude $j_c = 1 \times 10^{11}$ A/m^2 and a frequency $f = 19.47$ Hz. Hall resistance was measured vs applied external magnetic field B_{ext} oriented at an angle $\theta_B = 80^\circ$ and two different in-plane angles, $\varphi = 0^\circ$ and 90° [Fig. 1(c)]. The small out-of-plane field component was used to avoid domain nucleation at high fields and ensure coherent single-domain magnetization rotation. These measurements allow for the quantification of the effective magnetic fields generated by DL and FL-SOT as well as the PMA of the Co film. The first harmonic Hall resistance (R_f) is given by[5,7,9,13]

$$R_f = R_A \cos\theta + R_P \sin^2\theta \sin(2\varphi). \quad (1)$$

Here, R_A, R_P, θ, and φ correspond to the anomalous Hall resistance, the planar Hall resistance, and the polar and azimuthal angles of magnetization, respectively. R_f measured at $\varphi = 0^\circ$ is shown in Fig. 1(d) for both the poly-Co/Pt and epi-Co/Pt films. In this configuration, R_P is negligible and the signal is predominantly given by $R_A \cos\theta$, which allows us to quantify the magnetization angle $\theta = \cos^{-1}(R_f/R_A)$ accurately. Then, we estimate the effective perpendicular anisotropy field B_k by using a single-domain model in which $B_k = B_{ext}(\sin\theta_B/\sin\theta - \cos\theta_B/\cos\theta)$. The estimated B_k is nearly equal ($\sim$1.3 T) in both films, allowing us to compare SOTs by using both the harmonic and switching measurements directly.

The second harmonic Hall resistance R_{2f} is given by[4,9,31–33]

$$R_{2f} = (R_A \cos\theta - 2R_P \cos\theta \sin(2\varphi)) \frac{d\cos\theta}{dB_{ext}} \frac{B_\theta}{\sin(\theta_B - \theta)} + R_P \sin^2\theta \frac{2\cos 2\varphi}{B_{ext}\sin\theta_B} B_\varphi + R_{\nabla T}. \quad (2)$$

Here, B_θ and B_φ are the polar and azimuthal components of the SOT effective field. $R_{\nabla T}$ is the thermoelectric contribution to R_{2f}, which arises from the Joule heating induced thermal gradient along the

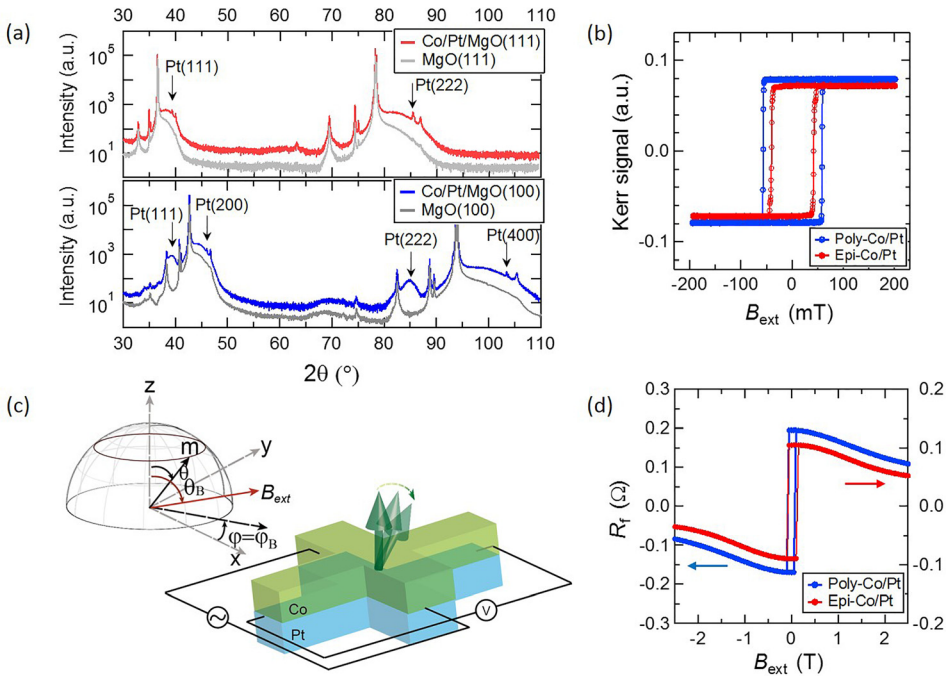

FIG. 1. (a) θ-2θ x-ray diffraction spectra of epi-Co/Pt (top panel) and poly-Co/Pt (bottom panel). The Pt peaks are labeled; the remaining unlabeled peaks correspond to the respective MgO substrate. (b) Out-of-plane magnetic hysteresis loops for poly-Co/Pt (blue line) and epi-Co/Pt (red line) obtained by polar magneto-optical Kerr effect measurements. (c) Brief schematics for harmonic Hall voltage measurements and its coordinate system. In this system, the azimuthal angle of magnetization **m** follows that of the external magnetic field B_{ext} ($\varphi = \varphi_B$). (d) First harmonic resistance R_f measured at $\theta_B = 80^\circ$, $\varphi = 0^\circ$ for poly-Co/Pt (blue line) and epi-Co/Pt (red line).

Published under license by AIP Publishing

out-of-plane direction.[4] To discuss the contribution of SOT in R_{2f}, $R_{2f,SOT}(=R_{2f}-R_{\nabla T})$ is obtained after subtraction of $R_{\nabla T}$ (see supplementary material for details). B_θ and B_φ are composed of effective fields induced by the DL-SOT B_{DL} and the FL-SOT B_{FL} whose contributions depend on B_{ext} and φ as follows:

$$B_\theta = B^{\theta}_{DL},\ B_\varphi = -B^{\varphi}_{FL}\ (\text{when } \varphi = 0^\circ), \tag{3}$$

$$B_\theta = -B^{\theta}_{FL}\cos\theta,\ B_\varphi = -B^{\varphi}_{DL}\cos\theta\ (\text{when } \varphi = 90^\circ). \tag{4}$$

Here, $B^{\theta}_{DL,FL} = B^{0}_{DL,FL} + B^{2}_{DL,FL}\sin^2\theta + B^{4}_{DL,FL}\sin^4\theta + \cdots$ and $B^{\varphi}_{DL,FL} \approx B^{0}_{DL,FL}$ are the polar and azimuthal components of B_{DL} and B_{FL}. Note that we include both the constant ($B^{0}_{DL,FL}$) and the magnetization angle dependent contributions ($B^{2}_{DL,FL}$, $B^{4}_{DL,FL}$, etc.) to the SOTs, as was first described in detail by Garello *et al.*[13] R_{2f} shows strong θ dependence due to the different dominant SOT contributions in these two geometries.

Figures 2(a) and 2(b) show $R_{2f,SOT}$ at $\varphi = 0^\circ$ and $\varphi = 90^\circ$ in poly-Co/Pt and epi-Co/Pt, respectively. $R_{2f,SOT}$ is odd (even) with respect to B_{ext}, when $\varphi = 0^\circ$ ($\varphi = 90^\circ$), as expected from the symmetries of DL and FL-SOT given above. Data were fitted to Eqs. (2)–(4) in order to extract B_{DL} and B_{FL} quantitatively. At a given φ, the effective fields B_θ and B_φ were recursively evaluated until they reproduced the measured $R_{2f,SOT}$ by taking into account the term arising from R_P.[13] Here, R_P in each sample was obtained by independent measurements by rotating the magnetization in the *xy* plane using a high in-plane magnetic field (see supplementary material).

The extracted B_{DL} and B_{FL} as a function of magnetization polar angle θ are reported in Figs. 2(c) and 2(d), respectively. We find that B_{DL} is larger in poly-Co/Pt than in epi-Co/Pt over the entire range of θ. On the other hand B_{FL} is similar in both poly-Co/Pt and epi-Co/Pt

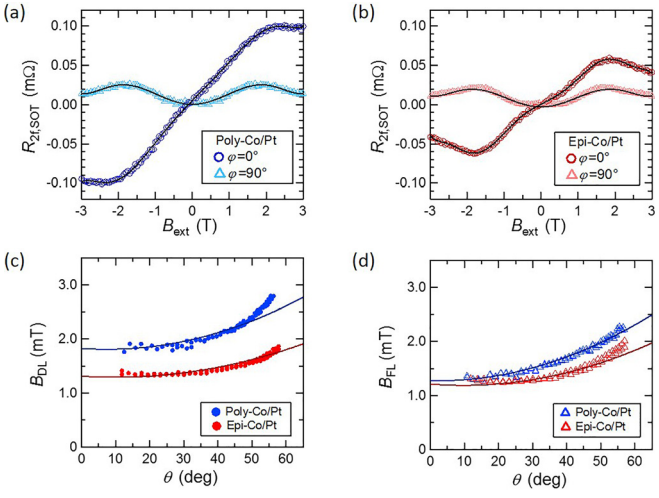

FIG. 2. (a) and (b) R_{2f} for poly-Co/Pt and epi-Co/Pt, respectively, measured with two applied field orientations φ_B. In (a) and (b), dark triangles and light circles correspond to R_{2f} along $\varphi_B = 0^\circ$ and $\varphi_B = 90^\circ$, respectively. Black lines show the R_{2f} reproduced based on iteratively-fitted B_{DL} and B_{FL}, as described in the main text. Note that in (a) and (b), the magnetothermal contributions are subtracted and a sample-dependent offset is removed. (c) and (d) Azimuthal magnetization angle θ dependence of the extracted B_{DL} and B_{FL}, respectively. The coefficient of $B^{0}_{DL,FL}$ is derived from the y-intercept by fitting lines based on $B^{\theta}_{DL,FL} = B^{0}_{DL,FL} + B^{2}_{DL,FL}\sin^2\theta + B^{4}_{DL,FL}\sin^4\theta$.

films. We fit the θ-dependence of the SOTs, which yield $B^{0}_{DL,poly} \approx 1.8$ mT, $B^{0}_{DL,epi} \approx 1.3$ mT and $B^{0}_{FL,poly} \approx B^{0}_{FL,epi} \approx 1.2$ mT for poly-Co/Pt and epi-Co/Pt, respectively. From these results, we computed the effective spin Hall angle, which includes the effects of interfacial spin transparency, using the relation $\theta_{SHE} = 2eM_S t_{co} B_{\mathrm{DL}}/\hbar j_c$, where e, M_S, t_{co}, and $\hbar$ are the electron charge, the saturation magnetization, the Co thickness and the reduced Planck constant, respectively.[34,35] We find $\theta_{SHE,poly} \approx 0.082$ for poly-Co/Pt and $\theta_{SHE,epi} \approx 0.059$ for epi-Co/Pt, in a range that has comparable values given in previous reports.[16,17,20,21,34,36] Consequently, we conclude that B^{0}_{DL} in epi-Co/Pt is approximately 1.3 times lower than that in poly-Co/Pt, whereas the FL-SOT shows no significant difference between the two samples.

Our observation that B_{DL} evidently depends on the crystal orientation of Pt, whereas B_{FL} does not, may indicate that different mechanisms are contributing to the two SOT effective fields. In the case of the DL-SOT, generally believed to be dominated by the spin Hall effect in the heavy metal, it has been broadly suggested that scattering events dominated by the Elliot-Yafet mechanism play an important role.[16,17,19,23,37,38] In the present films, the resistivity of the poly-Co/Pt film is notably larger than in the epi-Co/Pt film, which could suggest that different scattering rates give rise to different effective spin Hall angles. Thus, additional scatterings in the poly-Co/Pt film may lead to enhancement of the extrinsic contribution to the spin Hall angle, ultimately resulting in a larger DL-SOT in the poly-Co/Pt film. However, we note that other factors should also be considered for precise interpretation. For instance, the interface-generated SOTs and dependence of the spin Hall torque on the spin diffusion length also manifest in the effective θ_{SHE}, and these contributions could be different in the poly-Co/Pt and epi-Co/Pt films.[39–44] Although it is hard to separate bulk and interfacial contributions of SHE, the charge current density is more concentrated at the interface in poly-Co/Pt due to its high resistivity, and therefore interfacial SHE might be also enhanced. However, since the Pt thickness is significantly larger than the spin diffusion length, differences in these parameters are unlikely to be important in the experimentally-observed difference in θ_{SHE} between the two films.[17,23,38,45,46] The FL-SOT, by contrast, seems less sensitive to the bulk crystal orientation of Pt, suggesting that an interfacial mechanism may be dominant in giving rise to this torque component.

Finally, we performed current-induced magnetization switching to compare and contrast with the above findings. For these measurements, we sequentially inject 30 ms-long current pulses and then probe the out-of-plane magnetization by the Hall effect, with the amplitude of the current pulse incremented between each measurement. From this, we construct current-swept magnetization switching curves, as shown in the representative examples in Figs. 3(a) and 3(b). Measurements were performed with an applied field $B_{ext} = \pm 80$ mT along the current-flow axis, as required for deterministic switching. The observed switching polarities are the same for both samples and are consistent with the literature for Co/Pt. We define the critical current density j_{crit} to be the current density at which R_H crosses zero.

In Fig. 3(c), we plot $|j_{crit}|$ as a function of B_{ext}. We find that $|j_{crit}|$ gradually decreases with increasing B_{ext} as expected since the energy barrier for magnetization switching is lowered due to magnetization canting. We find that across the measured field range, $|j_{crit}|$ is approximately 1.3 times smaller for poly-Co/Pt compared to epi-Co/Pt. Since the anisotropy fields are nearly the same for these two samples, this

Published under license by AIP Publishing

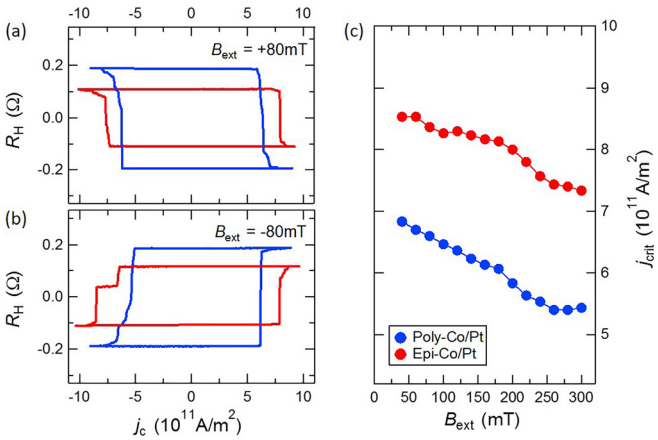

FIG. 3. (a) and (b) Current-induced magnetization switching as a function of injected current density j_c with (a) $B_{ext} = +80$ mT and (b) $B_{ext} = -80$ mT, oriented along the *x*-axis (current axis) in Fig. 1(c). Blue and red curves correspond to poly-Co/Pt and epi-Co/Pt, respectively. (c) Critical current required for magnetization switching $|j_{crit}|$ as a function of B_{ext}. Here, j_{crit} represents the current density at which R_H crosses zero and $|j_{crit}|$ is defined as the average between two switching behaviors up-to-down and down-to-up.

result suggests a weaker DL-SOT in epi-Co/Pt, in quantitative agreement with harmonic SOT measurements.

In conclusion, we investigated SOTs in perpendicularly magnetized epitaxial and polycrystalline Co/Pt bilayers by means of the harmonic Hall effect and current-induced switching measurements. We find that the DL-SOT in epi-Co/Pt is smaller by a factor of 1.3 compared to that of poly-Co/Pt, whereas the FL-SOT is comparable in both samples. As the DL-SOT is predominantly given by the SHE, which results from spin-dependent scattering in the bulk of Pt, we associate the difference in DL-SOT to the difference in the crystal orientations of Pt, which results in different scattering characteristics. In agreement with previous studies, our results suggest that B_{DL} is closely related to Pt resistivity; however, B_{FL} is not. Furthermore, the critical switching currents are different for the two films, with a higher switching efficiency observed in poly-Co/Pt, in good agreement with the DL-SOT estimation. This study highlights the effect of the crystal structure of the nonmagnetic heavy metal on SOTs, which may be important for understanding and engineering SOT-based spintronic devices.

See supplementary material for the XRD spectra of Pt/MgO and a detailed analysis to derive SOTs in epi-Co/Pt and poly-Co/Pt.

This work was supported by the Japan Society for the Promotion of Science with Grants-in-Aid 15H05699, 15H05854, and 15H02099 and by the National Science Foundation under Grant No. ECCS-1408172. The authors thank Hiromu Gamou, Keita Nakagawara, Professor Nobuki Tezuka, Maxwell Mann, Kohei Ueda, and David Bono for technical support.

REFERENCES

[1]I. M. Miron, K. Garello, G. Gaudin, P.-J. Zermatten, M. V. Costache, S. Auffret, S. Bandiera, B. Rodmacq, A. Schuhl, and P. Gambardella, Nature **476**, 189 (2011).
[2]I. M. Miron, T. Moore, H. Szambolics, L. D. Buda-Prejbeanu, S. Auffret, B. Rodmacq, S. Pizzini, J. Vogel, M. Bonfim, A. Schuhl, and G. Gaudin, Nat. Mater. **10**, 419 (2011).
[3]L. Liu, C.-F. Pai, Y. Li, H. W. Tseng, D. C. Ralph, and R. A. Buhrman, Science **336**, 555 (2012).
[4]C. O. Avci, K. Garello, M. Gabureac, A. Ghosh, A. Fuhrer, S. F. Alvarado, and P. Gambardella, Phys. Rev. B **90**, 224427 (2014).
[5]M. Hayashi, J. Kim, M. Yamanouchi, and H. Ohno, Phys. Rev. B **89**, 144425 (2014).
[6]S. Fukami, T. Anekawa, C. Zhang, and H. Ohno, Nat. Nanotechnol. **11**, 621 (2016).
[7]J. Kim, J. Sinha, M. Hayashi, M. Yamanouchi, S. Fukami, T. Suzuki, S. Mitani, and H. Ohno, Nat. Mater. **12**, 240 (2013).
[8]C.-F. Pai, L. Liu, Y. Li, H. W. Tseng, D. C. Ralph, and R. A. Buhrman, Appl. Phys. Lett. **101**, 122404 (2012).
[9]A. Ghosh, K. Garello, C. O. Avci, M. Gabureac, and P. Gambardella, Phys. Rev. A **7**, 014004 (2017).
[10]S. Woo, M. Mann, A. J. Tan, L. Caretta, and G. S. D. Beach, Appl. Phys. Lett. **105**, 212404 (2014).
[11]S. Emori, T. Nan, A. M. Belkessam, X. Wang, A. D. Matyushov, C. J. Babroski, Y. Gao, H. Lin, and N. X. Sun, Phys. Rev. B **93**, 180402(R) (2016).
[12]J. Yu, X. Qiu, Y. Wu, J. Yoon, P. Deorani, J. M. Besbas, A. Manchon, and H. Yang, Sci. Rep. **6**, 32629 (2016).
[13]K. Garello, I. M. Miron, C. O. Avci, F. Freimuth, Y. Mokrousov, S. Blügel, S. Auffret, O. Boulle, G. Gaudin, and P. Gambardella, Nat. Nanotechnol. **8**, 587 (2013).
[14]M. Baumgartner, K. Garello, J. Mendil, C. O. Avci, E. Grimaldi, C. Murer, J. Feng, M. Gabureac, C. Stamm, Y. Acremann, S. Finizio, S. Wintz, J. Raabe, and P. Gambardella, Nat. Nanotechnol. **12**, 980 (2017).
[15]S. Emori, U. Bauer, S. M. Ahn, E. Martinez, and G. S. D. Beach, Nat. Mater. **12**, 611 (2013).
[16]J. W. Lee, Y. Oh, S. Park, A. I. Figueroa, G. Van Der Laan, G. Go, K. Lee, and B. Park, Phys. Rev. B **96**, 064405 (2017).
[17]M. Nguyen, D. C. Ralph, and R. A. Buhrman, Phys. Rev. Lett. **116**, 126601 (2016).
[18]A. Hoffmann, IEEE Trans. Magn. **49**, 5172 (2013).
[19]M. Morota, Y. Niimi, K. Ohnishi, D. H. Wei, T. Tanaka, H. Kontani, T. Kimura, and Y. Otani, Phys. Rev. B **83**, 174405 (2011).
[20]L. Liu, T. Moriyama, D. C. Ralph, and R. A. Buhrman, Phys. Rev. Lett. **106**, 036601 (2011).
[21]K. Ando, S. Takahashi, J. Ieda, Y. Kajiwara, H. Nakayama, T. Yoshino, K. Harii, Y. Fujikawa, M. Matsuo, S. Maekawa, and E. Saitoh, J. Appl. Phys. **109**, 103913 (2011).
[22]L. Liu, O. J. Lee, T. J. Gudmundsen, D. C. Ralph, and R. A. Buhrman, Phys. Rev. Lett. **109**, 096602 (2012).
[23]E. Sagasta, Y. Omori, M. Isasa, M. Gradhand, L. E. Hueso, Y. Niimi, Y. Otani, and F. Casanova, Phys. Rev. B **94**, 060412(R) (2016).
[24]J. Ryu, M. Kohda, and J. Nitta, Phys. Rev. Lett. **116**, 256802 (2016).
[25]N. H. Long, P. Mavropoulos, D. S. Bauer, B. Zimmermann, Y. Mokrousov, and S. Blügel, Phys. Rev. B **94**, 180406(R) (2016).
[26]R. Freeman, A. Zholud, Z. Dun, H. Zhou, and S. Urazhdin, Phys. Rev. Lett. **120**, 67204 (2018).
[27]R. J. Elliott, Phys. Rev. **96**, 266 (1954).
[28]Y. Yafet, Phys. Rev. **85**, 478 (1952).
[29]B. M. Lairson, M. R. Visokay, R. Sinclair, S. Hagstrom, and B. M. Clemens, Appl. Phys. Lett. **61**, 1390 (1992).
[30]P. C. McIntyre, C. J. Maggiore, and M. Nastasi, J. Appl. Phys. **77**, 6201 (1995).
[31]K. Garello, C. O. Avci, I. M. Miron, M. Baumgartner, A. Ghosh, S. Auffret, G. Gaudin, P. Gambardella, K. Garello, O. Avci, I. M. Miron, and M. Baumgartner, Appl. Phys. Lett. **105**, 212402 (2014).
[32]C. O. Avci, K. Garello, C. Nistor, S. Godey, A. Mugarza, A. Barla, M. Valvidares, E. Pellegrin, A. Ghosh, I. M. Miron, O. Boulle, S. Auffret, G. Gaudin, and P. Gambardella, Phys. Rev. B **89**, 214419 (2014).
[33]D. J. Kim, C. Y. Jeon, J. G. Choi, J. W. Lee, S. Surabhi, J. R. Jeong, K. J. Lee, and B. G. Park, Nat. Commun. **8**, 1400 (2017).
[34]C. F. Pai, Y. Ou, L. H. Vilela-Leão, D. C. Ralph, and R. A. Buhrman, Phys. Rev. B **92**, 064426 (2015).

Published under license by AIP Publishing

[35]A. V. Khvalkovskiy, V. Cros, D. Apalkov, V. Nikitin, M. Krounbi, K. A. Zvezdin, A. Anane, J. Grollier, and A. Fert, Phys. Rev. B **87**, 020402(R) (2013).
[36]W. Zhang, W. Han, X. Jiang, S. Yang, and S. S. P. Parkin, Nat. Phys. **11**, 496 (2015).
[37]Y. Niimi, D. Wei, H. Idzuchi, T. Wakamura, T. Kato, and Y. Otani, Phys. Rev. Lett. **110**, 016805 (2013).
[38]A. J. Berger, E. R. J. Edwards, H. T. Nembach, O. Karis, M. Weiler, and T. J. Silva, Phys. Rev. B **98**, 024402 (2018).
[39]A. Manchon and S. Zhang, Phys. Rev. B **79**, 094422 (2009).
[40]P. M. Haney, H. W. Lee, K. J. Lee, A. Manchon, and M. D. Stiles, Phys. Rev. B **88**, 214417 (2013).
[41]F. Freimuth, S. Blügel, and Y. Mokrousov, Phys. Rev. B **92**, 064415 (2015).
[42]V. P. Amin and M. D. Stiles, Phys. Rev. B **94**, 104420 (2016).
[43]L. Wang, R. J. H. Wesselink, Y. Liu, Z. Yuan, K. Xia, and P. J. Kelly, Phys. Rev. Lett. **116**, 196602 (2016).
[44]V. P. Amin, J. Zemen, and M. D. Stiles, Phys. Rev. Lett. **121**, 136805 (2018).
[45]L. Ma, L. Lang, J. Kim, Z. Yuan, R. Wu, S. Zhou, and X. Qiu, Phys. Rev. B **98**, 224424 (2018).
[46]M. Caminale, A. Ghosh, S. Auffret, U. Ebels, K. Ollefs, F. Wilhelm, A. Rogalev, and W. E. Bailey, Phys. Rev. B **94**, 014414 (2016).

Published under license by AIP Publishing